ACS APPLIED MATERIALS & INTERFACES

Research Article

www.acsami.org

Effect of Fluorene Groups on the Properties of Multiblock Poly(arylene ether sulfone)s-Based Anion-Exchange Membranes

Pei Yu Xu, Ke Zhou, Guang Lu Han, Qiu Gen Zhang, Ai Mei Zhu, and Qing Lin Liu*

Department of Chemical & Biochemical Engineering, College of Chemistry & Chemical Engineering, Xiamen University, Xiamen 361005, Fujian, China

Supporting Information

ABSTRACT: Two kinds of novel multiblock poly(arylene ether sulfone)s were synthesized via block copolycondensation of telechelic oligomers as a starting material for the preparation of anion-exchange membranes (AEMs). The as-synthesized copolymers have extremely similar main chains. The difference is that the benzylmethyl groups for one are located on the fluorene−sulfone segments and they are located on the isopropylidene−sulfone segments for the other. The benzylmethyl moieties served as precursors to cationic sites and were brominated using *N*-bromosuccinimide (NBS) and then quaternized with *N*,*N*,*N*′,*N*′-tetramethyl-1,6-diaminohexane (TMHDA). Controlled bromination and quaternization at specific positions of the benzylmethy-containing fluorene−sulfone segments and isopropylidene−sulfone segments can be achieved. ^{1}H NMR spectroscopy, Fourier transform infrared spectroscopy, and gel permeation chromatography were used to characterize the as-synthesized copolymers. Distinct microphase separation in the as-prepared AEMs was observed using small-angle X-ray scattering and transmission electron microscopy. The AEM containing fluorene−sulfone segments (IEC = 1.89 meq·g^{-1}) showed higher ionic conductivity and methanol permeability than that containing isopropylidene−sulfone segments (IEC = 2.03 meq·g^{-1}). Moreover, the former showed better alkaline stability than the latter.

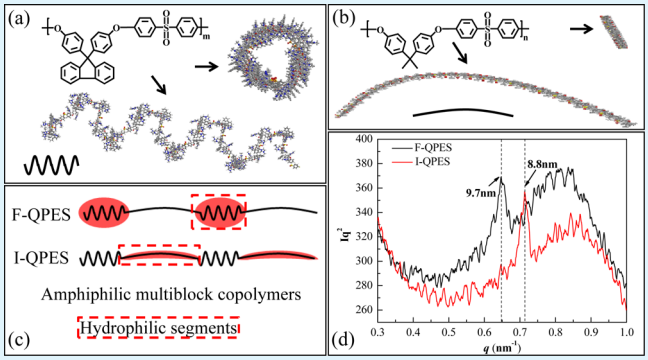

KEYWORDS: *anion-exchange membranes, poly(arylene ether sulfone), microphase separation, ionic conductivity, alkaline stability, methanol permeability*

1. INTRODUCTION

Polymer electrolyte fuel cells (PEFCs) using proton-exchange membranes (PEMs) as the electrolyte have attracted considerable attention because of their high energy conversion efficiency, low environmental burden, and potential for use in a variety of applications.[1] State-of-the-art PEMs are made from perfluorinated sulfonic acid polymers (such as Nafion, Du Pont) and exhibit excellent mechanical strength, chemical and thermal stability, and high proton conductivity. However, these advantages come with several drawbacks such as high production cost, environmental incompatibility, and limited operation temperature in fuel cells. Moreover, precious-metal-based electrocatalysts such as Pt are essential under strongly acidic conditions.[2−5] Recently, alkaline fuel cells (AFCs), which utilize anion-exchange membranes (AEMs) as the electrolyte, have emerged as an alternative because of their faster oxygen reduction reaction kinetics, higher catalytic activity, lower methanol permeability in alkaline media, and larger number of options for cathode catalysts based on the abundance of transition metals such as nickel.[6,7]

Because the existing AEMs are not as conductive and stable as PEMs, a growing effort is underway to develop better AEM materials that simultaneously possess high hydroxide conductivity, good mechanical properties, and robust alkaline stability under fuel cell (FC) operating conditions. Aromatic polymers are thermally and chemically stable, which make them attractive as a component of AEMs. Of the aromatic polymers, poly(arylene ether sulfone) (PES) is considered to be a promising material for AEM FC applications because of its high glass transition temperature as well as its excellent chemical and thermal stability.[8] A number of AEMs based on PES containing ammonium, imidazorium, or guanidinium groups[9−13] have been investigated over the last few years. Recently, fluorene-containing PESs have attracted considerable attention for both PEMs and AEMs. Various types of fluorene-containing poly(arylene ether sulfone) PEMs have demonstrated some attractive properties such as chemical, thermal, and mechanical stability and low methanol permeability.[14−18] Tanaka et al.[19−21] developed a series of random and multiblock fluorene-containing PES AEMs with a high ammonium density. The well-controlled multiblock copolymers with a hydrophilic/hydrophobic phase-separated morphology were more effective

Received: January 24, 2014
Accepted: April 8, 2014
Published: April 8, 2014

   dx.doi.org/10.1021/am5017599 | ACS Appl. Mater. Interfaces 2014, 6, 6776−6785

Scheme 1. Synthesis of Oligomer-OH, Oligomer-F, MPES, BPES, and QPES

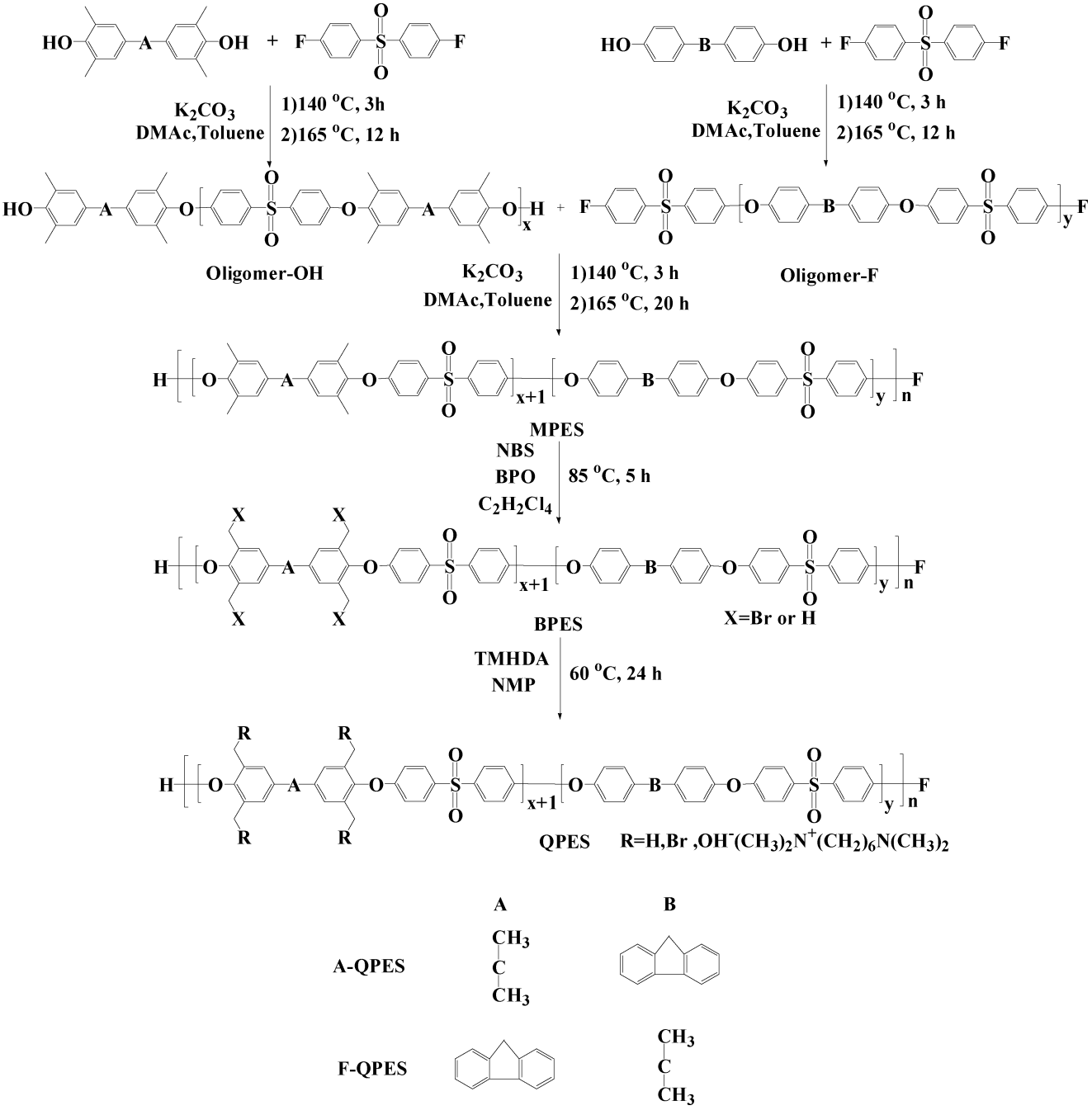

at improving the ionic conductivity of AEMs than were the random-structured copolymer membranes.

Miyatake et al.[22] assumed that introducing bulky and rigid fluorene groups into the main chain could force each polymer chain apart to produce large interchain separations (free volume) in which water molecules could be confined. However, this hypothesis was based on fluorene groups being introduced into amphiphilic random copolymers. Currently, there are not any reports on the differences between fluorene groups that act purely as a hydrophilic segment or as a hydrophobic segment in multiblock copolymers. In this work, two kinds of multiblock PESs were synthesized via block copolycondensation of telechelic oligomers. The as-synthesized copolymers have extremely similar main chains; the difference between them is that the benzylmethyl moieties that served as precursors to cationic sites are located on the fluorene−sulfone segments for one copolymer and are located on the isopropylidene−sulfone segments for the other. Bromination of the benzylmethyl groups followed by quaternization of the AEMs containing hydrophilic quaternized ammonio-substituted fluorene−sulfone segments and hydrophobic isopropylidene−sulfone segments were prepared. Similarly, those containing hydrophilic quaternized ammonio-substituted isopropylidene−sulfone segments and hydrophobic fluorene−sulfone segments were also prepared. The influence of the fluorene groups that were introduced into the backbone on the performance of the membrane, including water uptake, ionic conductivity,

dx.doi.org/10.1021/am5017599 | ACS Appl. Mater. Interfaces 2014, 6, 6776−6785

mechanical properties, methanol permeability, and thermal and alkaline stability, was fully evaluated.

2. EXPERIMENTAL SECTION

2.1. Materials. 9-Fluorenone (99%, Aldrich, USA), silicotungstic acid (AR, Aladdin, China), 2,6-dimethylphenol (99%, Aladdin, China), bis(4-fluorophenyl) sulfone (FPS) (99.0%, TCI, Japan), 9,9′-bis(4-hydroxyphenyl) fluorene (BHF) (99%, Matrix, USA), 4,4-isopropylidenebis (2,6-dimethylphenol) (DMBHA) (98%, Aldrich, USA), bisphenol A (BHA) (97%, Aldrich, USA), and TMHDA (98.0%, TCI, Japan) were used as received. Toluene and *N*,*N*-dimethylacetamide (DMAc) were stirred over CaH_2 for 24 h, distilled under reduced pressure, and stored over 4 Å molecular sieves. Benzoyl peroxide (BPO) was supplied from Tianjin Guangfu Fine Chemical Research Institute (China) and was recrystallized from chloroform. All other chemicals were supplied from Shanghai Chemical Reagent Store (China) and used without further purification.

2.2. Preparation of Anion-Exchange Membranes. *2.2.1. Synthesis of the Monomer 9,9′-Bis(4-hydroxy-3,5-dimethylphenyl)-fluorene (DMBHF).* DMBHF was synthesized from 9-fluorenone and 2,6-dimethylphenol by a method described in the literature.[23] Fluorenone (18.20 g, 0.10 mol), an excess of 2,6-dimethylphenol (61.08 g, 0.50 mol), and silicotungstic acid (1.2 g) were introduced into a 250 mL three-necked round-bottomed flask equipped with a magnetic stirrer, a condenser, and a thermometer. The mixture was stirred at 70 °C for 4 h under reduced pressure (1.3×10^3 Pa). A NaOH solution (1.2 g of 29 wt %) was then added to stop the reaction. One-hundred twenty five grams of toluene and 35 g of deionized (DI) water were added into the mixture under vigorous stirring, leading to phase separation. The aqueous phase was removed using a separatory funnel. The organic phase was washed twice with DI water and cooled to 10 °C to crystallization. After filtration, the residue was washed with DI water to yield a crude product, which was further recrystallized from toluene twice to obtain a pure white DMBHF powder (yield: 78%).

2.2.2. Synthesis of Multiblock Benzylmethyl-Containing Poly(arylene ether sulfone) (MPESs). Two kinds of precursors with benzylmethyl on different segments of the similar main chain structure (F-MPES and I-MPES) were prepared by nucleophilic substitution polycondensation of the separately synthesized telechelic oligomers, as shown in Scheme 1.[19] F denotes benzylmethyl residing on the fluorene−sulfone segment, and I denotes benzylmethyl residing on the isopropylidene−sulfone segment. A typical procedure for the synthesis of F-MPES was as follows. The hydrophilic OH-terminated telechelic oligomer (oligomer-OH) fx26 was synthesized first, where f denotes the fluorene group, x denotes the terminal hydroxyl group, and the number after x denotes the degree of polymerization of the oligomers. DMBHF (4.2278 g, 10.4 mmol), FPS (2.5425 g, 10 mmol), potassium carbonate (3.5929 g, 26 mmol), DMAc (30 mL), and toluene (15 mL) were placed into a 100 mL round-bottomed flask equipped with a Dean−Stark trap, a condenser, a magnetic stirrer, and a gas inlet and outlet. The polymerization reaction was carried out at 140 °C under nitrogen flow for 3 h before removing the Dean−Stark trap. Then, the temperature was raised to 165 °C, and the reaction was continued for another 12 h to obtain a black viscous mixture. The mixture was cooled to room temperature and poured into 200 mL of an aqueous methanol solution (methanol/deionized water = 1:1, v/v) followed by magnetic stirring in the aqueous methanol solution at 80 °C for another 4 h and subsequent filtration to yield a crude solid product. After Soxhlet extraction of the solid with acetone for 12 h and vacuum drying at 80 °C for 24 h, we obtained a gray solid product with hydroxy-containing terminal groups. The degree of polymerization of the hydrophilic oligomer was determined to be 25.7 from GPC. The ix26 (i denotes the isopropylidene group) oligomer was synthesized as mentioned above, replacing DMBHF with DMBHA, and the degree of polymerization was determined to be 26.3 from GPC.

Similar to the hydrophilic oligomer, the hydrophobic F-terminated telechelic oligomer (oligomer-F) iy23 was synthesized, where y denotes the terminal fluoride group, and the number after y denotes the degree of polymerization of the hydrophobic blocks. BHA (3.5041 g, 10 mmol), FPS (2.6442 g, 10.4 mmol), potassium carbonate (3.5929 g, 26 mmol), DMAc (30 mL), and toluene (15 mL) were fed into a 100 mL round-bottomed flask equipped with a Dean−Stark trap, a condenser, a magnetic stirrer, and a gas inlet and outlet. Using similar protocols and reaction conditions as those for oligomer-OH preparation, the polymerization reaction was carried out, yielding a white viscous mixture. After the same purification treatments, a white solid product carrying F-containing terminal groups was obtained. The degree of polymerization of the hydrophobic oligomer was determined to be 23.3 from GPC. The fy27 oligomer was synthesized as mentioned above, replacing BHA with BHF, and the degree of polymerization was determined to be 27.0 from GPC.

Synthesis of MPESs via block copolymerization was carried out as follows (Scheme 1). An equimolar amount of oligomers fx26 and iy23 was copolymerized at 140 °C for 3 h and then at 165°C for another 20 h in the presence of potassium carbonate under a nitrogen atmosphere. DMAc was used as the solvent in the reaction, and was toluene used as an azeotropic solvent for water removal. After the polymerization, extra DMAc was added to reduce the viscosity. The mixture was cooled to room temperature and poured into 200 mL of an aqueous methanol solution (methanol/deionized water = 1:1, v/v) followed by magnetic stirring in the aqueous methanol solution at 80 °C for another 4 h and subsequent filtration to yield a crude solid product. After Soxhlet extracting the solid with acetone for 12 h and drying at 80 °C for 24 h under vacuum, we obtained a gray solid target product of F-MPES. I-MPES was synthesized as mentioned above, replacing fx26 and iy23 with ix26 and fy27, respectively.

2.2.3. Bromination of MPESs. The radical substitution bromination reaction of the benzylmethyl-bearing poly(sulfone)s was carried out in 1,1,2,2-tetrachloroethane (TCE) using NBS and benzoyl peroxide (BPO) as the bromination agent and initiator, respectively (Scheme 1). A typical procedure for the synthesis of F-BPES was as follows. F-MPES (1.0000 g) and TCE (20 mL) were charged into a 100 mL three-necked round-bottomed flask equipped with a condenser, a magnetic stirrer, and a gas inlet and outlet. After being dissolved completely, 0.6307 g of NBS and 0.0429 g of BPO were added. The mixture was heated at 85°C under nitrogen for 5 h. The mixture was cooled to room temperature and then poured into 200 mL of methanol to give a precipitate followed by filtration to yield a crude solid. After Soxhlet extraction of the crude product with acetone for 12 h and vacuum drying at 80 °C for 24 h, we obtained a yellow solid. The product is termed F-BPES, where B denotes the bromination reaction.

2.2.4. Quaternization of BPES and Membrane Formation. The S_N2 substitution quaternization reaction was carried out using TMHDA to aminate the bromomethyl groups (Scheme 1). TMHDA was chosen as a quaternization agent because it shows better alkaline stability than others.[24] A typical procedure for F-QPES was carried out as follows: 1.0000 g of F-BPES was completely dissolved in 25 mL of *N*-methyl-2-pyrrolidone (NMP) by magnetic stirring at 60 °C. The solution was added dropwise into 5 mL of a NMP solution containing TMHDA to avoid the cross-linking reaction. The molar ratio of TMHDA to the $-CH_2Br$ groups in F-BPES was controlled at 3:1 to ensure that $-CH_2Br$ was completely converted into the desired quaternary ammonium group. After the reaction proceeded for 24 h, the solution was poured into 100 mL of methanol followed by filtration to yield a precipitate. It was further Soxhlet extracted with acetone for 12 h to remove the excess TMHDA and vacuum dried at 60 °C for 24 h to obtain a brown solid. The solid (1.0000 g) was completely dissolved in 25 mL of NMP followed by filtration using a 0.45 μm PTFE membrane to make a solution. Under vacuum, the resulting solution was cast onto clean glass plates and heated at 60 °C for 24 h to obtain transparent membranes that were 40 ± 3 μm in thickness. The membrane is termed F-QPES, where Q denotes the quaternization reaction.

2.3. Characterization. *2.3.1. ^{1}H NMR Spectroscopy.* An Avancell 500 MHz spectrometer (Bruker, Switzerland) was used to record ^{1}H NMR spectra. Deuterated chloroform ($CDCl_3$-*d*) was used as the solvent, and tetramethylsilane (TMS) served as the internal reference.

2.3.2. Gel Permeation Chromatography (GPC) Measurement. A GPC (Waters, USA) equipped with a Waters 1515 isocratic HPLC pump was used for the measurement of the apparent molecular weight. Tetrahydrofuran (THF) was used as the eluent at a flow rate of 1.0 mL·min^{-1}. Three Styragel columns (Waters HT4, HT5E, and HT6) and a Waters 2414 refractive index detector set to 30 °C were used. The molecular weight was calibrated using standard polystyrene samples.

2.3.3. FTIR Spectroscopy. FTIR spectra of the membrane samples were recorded in the range 4000−500 cm^{-1} with a resolution of 4 cm^{-1} using a Nicolet Avatar 330 spectrophotometer (Thermo Electron Corporation, USA).

2.3.4. Small-Angle X-ray Scattering (SAXS). SAXS patterns were recorded on a SAXSess-MC2 X-ray diffractometer (Anton Paar, Austria). The range of scattering vectors ($q = 4\pi \sin \theta/\lambda_i$) is from 0.3 to 1.0 nm^{-1}, where λ_i and 2θ are the incident wavelength and the total scattering angle, respectively. Because the peak position (q_{MAX}) is generally recognized to be the hydrophilic aggregates, the Bragg distance (d_{MAX}), calculated from the equation $d_{MAX} = 2\pi/q_{MAX}$, is assumed to represent the size of the hydrophilic aggregates in the membranes.[25]

2.3.5. Transmission Electron Microscopy (TEM). TEM characterization was performed on a JEM-1230 electron microscope (JEOL, Japan) with an operating voltage of 120 kV. The membrane was first stained with tungstate ions by immersing in a 1.0 M aqueous sodium tungstate solution for 24 h. After washing with deionized water several times and drying in a vacuum oven at 60 °C for 24 h, the membrane was embedded in an epoxy resin, ultramicrotomed into 60 nm thin sections with a diamond knife, and placed on copper grids for observation.

2.3.6. Scanning Electron Microscopy (SEM). A field-emission scanning electron microscope (S-4800, Hitachi, Japan) was used to characterize the morphology and microstructure of the membranes. All of the samples were fractured in liquid nitrogen and then sputtered with gold before observation.

2.3.7. Thermal Stability. The thermal stability of the membranes was evaluated using a thermogravimetric analyzer (SDQT600, TA, USA). The testing was performed in the temperature range 30−700 °C at a heating rate of 10 °C·min^{-1} under an air atmosphere.

2.3.8. Water Uptake (WU). The WU was examined using a quartz spring balance after the membranes were dried at 60 °C under vacuum for 24 h. The original length of the quartz spring is L_1. After the dry membrane was loaded, the length extended to L_2. The quartz spring with the dry membrane was then fixed on a ground glass stopper that was fixed on the top of an inner glass cylinder with a sealed bottom, and 50 mL of DI water was put into the bottom and heated to form a stable and saturated vapor pressure. Circulating water was used between the inner and the outer glass cylinders to control the temperature. The water vapor made the membrane swell. After 48 h, the length of the quartz spring loaded with the swollen membrane is L_3. The WU of the membrane can be calculated by Hooke's law

$$\mathrm{WU} = \frac{kL_3 - kL_2}{kL_2 - kL_1} \times 100\% = \frac{L_3 - L_2}{L_2 - L_1} \times 100\% \quad (1)$$

where k is the elasticity coefficient of the quartz spring.

2.3.9. Swelling Ratio (SR). The SR of the membrane was measured in the plane direction and is calculated by

$$\mathrm{SR} = \frac{L_w \times W_w - L_d \times W_d}{L_d \times W_d} \times 100\% \quad (2)$$

where L_w and L_d are the length of the wet and the dried membranes, respectively, and W_w and W_d are the width of the wet and the dried membranes, respectively.

2.3.10. Ionic Exchange Capacity (IEC). The classical back titration method was employed to determine the IEC of the membrane. The membrane was dried in hydroxide form at 60 °C under vacuum for 24 h and immersed into 10 mL of a 0.1 M HCl solution for 24 h to ensure that all OH^- was ion-exchanged by Cl^-. The solution and the membrane were then back titrated with a 0.05 M KOH solution. The IEC values (meq·g^{-1}) are calculated by

$$\mathrm{IEC} = \frac{M_{o,HCl} - M_{e,HCl}}{m_d} \times 100\% \quad (3)$$

where $M_{o,HCl}$ and $M_{e,HCl}$ (M) are the milliequivalents (meq) of HCl required before and after equilibrium, respectively, m_d is the mass of the dried membranes (g).

2.3.11. Ionic Conductivity. A Parstat 263 electrochemical workstation (Princeton Advanced Technology, USA) was used to measure the resistance of the membrane samples by the two-electrode ac impedance spectroscopy method.[26] The test is performed at a constant voltage of 10.0 mV in the frequency range from 100 mHz to 100 kHz at temperatures of 30−80 °C. Before testing, the hydroxide-form membranes were hydrated in deionized water for at least 48 h. The testing device with a 1 × 2 cm^2 membrane was clamped between two stainless steel electrodes and then placed in a chamber with DI water to maintain a relative humidity (RH) of 100% during the measurements. The ionic conductivity, σ (S·cm^{-1}), is calculated as follows

$$\sigma = \frac{l}{AR} \quad (4)$$

where l (cm) is the distance between the two electrodes and A (cm^2) is the cross-sectional area of the tested membrane.

2.3.12. Mechanical Property. The mechanical properties of the membranes were studied using a universal testing machine (Instron 3343 testing system) with a crosshead speed of 10 mm·min^{-1} at room temperature and 60% RH. A 15 mm wide membrane was kept in DI water at room temperature overnight and was taken out to remove the surface water using a tissue before the measurements.

2.3.13. Methanol Permeability. A home-made diffusion setup composed of two identical cells (25 cm^3) separated by a membrane was used[26] to measure the methanol permeability of the membrane. Cells A and B were filled with 20 mL of a 2 M aqueous methanol solution and 20 mL of DI water, respectively. The variation of the methanol concentration with time (t) in the water side was measured at regular intervals by gas chromatography (GC-950, Shanghai Haixin Chromatographic Instruments Co., Ltd). The transfer of methanol in the membrane was described using the solution-diffusion model. As implied in the mechanism, methanol permeability (P) is the product of the diffusion coefficient (D) and the solubility coefficient (H), $P = DH$. The relationship between P and the methanol concentration on the water side was obtained by taking into consideration the diffusion only along the direction of the thickness of the membrane.

$$C_B(t) = \frac{A_m}{V_B}\frac{DH}{L}C_A(t - t_0) \quad (5)$$

where C_A and C_B (M) are the methanol concentration of cells A and B, respectively, V_B is the solution volume of the permeate compartment (cm^3), A_m is the effective area of the membrane (cm^2), and L is the membrane thickness (cm).

The methanol permeability is calculated from the slope of the straight line (α) by

$$P = \alpha\frac{V_B}{A_m}\frac{L}{C_A} \quad (6)$$

2.3.14. Alkaline Stability. To determine the alkaline stability of the AEMs, the membranes were immersed in a 2 M NaOH solution at 60 °C for 48−480 h (with a time interval of 48 h) and were then immersed in DI water for over 24 h before testing at 30 °C.

3. RESULTS AND DISCUSSION

3.1. Synthesis and Characterization of Oligomers. A series of telechelic oligomers (fx26, ix26, fy27, and iy23) was synthesized by adjusting the feed molar ratio of the hydroxy-containing monomers to the fluorine-containing monomers to

control the length of telechelic oligomers, as shown in Scheme 1. Different end-group oligomers were obtained and characterized by ^{1}H NMR and GPC (see the Supporting Information). Figures S1 and S2 (Supporting Information) show the ^{1}H NMR spectra of fx26 and ix26. Protons attached to the OH-terminated phenylene rings (a′, b′, i′, j′, and k′) appeared and were distinguished from those attached to the oxyphenylene rings (a, b, i, j, and k). The ^{1}H NMR spectra of fy27 and iy23 are shown in Figures S3 and S4 (Supporting Information), respectively. Protons attached to the F-terminated phenylene rings (g′, h′, l′, and m′) appeared and were distinguished from those attached to the sulfonyl phenyleneoxy rings (g, h, l, and m). The experimental values of x and y were calculated from the GPC data for these oligomers, as shown in Table S1 (Supporting Information). They are close to the target value. All the above results prove the formation of the telechelic oligomers.

3.2. Synthesis and Characterization of Block Copolymers. Two kinds of multiblock copolymers (F-MPES and I-MPES) were synthesized by a coupling reaction between OH- and F-telechelic oligomers (Scheme 1). The coupling reaction was conducted between the phenoxide end groups on the hydrophilic oligomers and the fluorine on the hydrophobic oligomers using an equimolar amount of hydrophobic and hydrophilic oligomers in an anhydrous DMAc/toluene mixture. The resulting copolymers have the same main chain structure, but the benzylmethyl group, which can be modified, is located on different segments. The obtained block copolymers were characterized by ^{1}H NMR and GPC. A comparison of the ^{1}H NMR spectra of the F-MPES (Figure 1) and I-MPES (Figure 2) block copolymers with those of the telechelic oligomers (Figures S1−S4, Supporting Information) reveals the disappearance of the protons attached to the OH-terminated phenylene rings (a′, b′, i′, j′, and k′) and the F-terminated phenylene rings (g′, h′, l′, and m′) as well as the presence of other peaks that were well-assigned to the chemical structure of the oligomers. As summarized in Table 1, the ratio of the experimentally determined length of the hydrophilic segment to that of the hydrophobic segment is close to the expected value, and each of the block copolymers has a sufficiently high molecular weight (M_n > 12 kDa and M_w > 20 kDa) for membrane formation. All of these data support the formation of block copolymers.

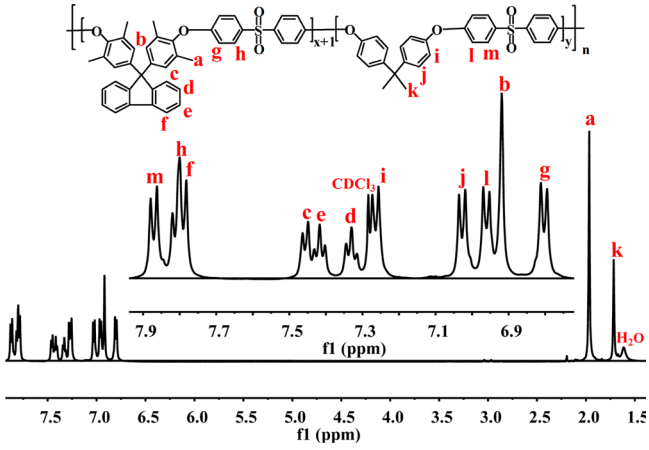

Figure 1. ^{1}H NMR spectrum of the F-MPES block copolymer.

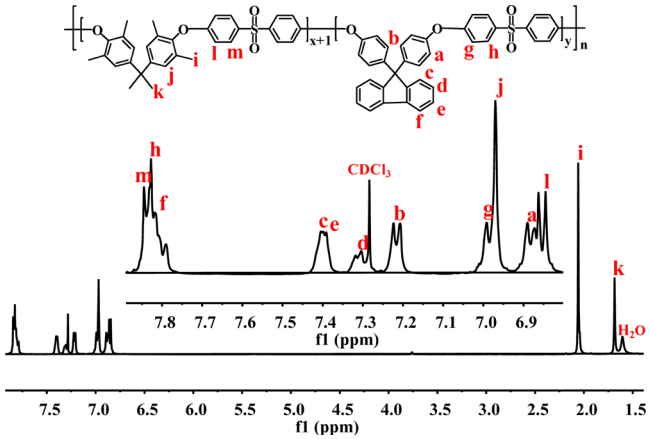

Figure 2. ^{1}H NMR spectrum of the I-MPES block copolymer.

3.3. Synthesis and Characterization of Brominated Block Copolymers. The synthesis of the BPESs in which $-CH_3$ was converted to $-CH_2Br$ was carried out in TCE using NBS as the brominating agent and BPO as the initiator. The chemical structures of F-BPES (Figure 3) and I-BPES (Figure 4) were analyzed by ^{1}H NMR. A comparison of the above spectra with those of F-MPES (Figure 1) and I-MPES (Figure 2) reveals a new peak that represents the methylene protons of the bromomethyl groups appearing at 4.07−4.24 ppm, and the peak associated with the methyl decreased in size. Successful bromination of the benzyl on the polymer is thus confirmed. As shown in Table 1, the conversion of the methyl groups of MPESs to bromomethyl groups can be estimated from the integral area ratio of the brominated benzyl peaks to the (brominated benzyl peaks + unreacted benzyl peaks); the degree of bromination of F-BPES and I-BPES was 81.41% and 82.11%, respectively.

3.4. Quaternization, Membrane Formation, and FTIR Spectra. QPESs were prepared via the reaction of the intermediate BPESs with TMHDA. FTIR was used to examine the functional groups of the MPESs, BPESs, and QPESs to ensure that the corresponding reactions took place as expected. The peak at 1240 cm^{-1} in the spectrum of F-MPES (Figure 5a) is associated with the Ar−O bond, suggesting the successful synthesis of F-MPES. In the spectrum of F-BPES (Figure 5c), the band at 628 cm^{-1} was assigned to the C−Br stretching vibration. Similar to the QPES analogues (Figure 5e), the new characteristic peak at 1568 cm^{-1} was attributed to the C−N stretching vibration, the new broad peak at 3412 cm^{-1} was attributed to the O−H stretching vibration, and the peak associated with the C−Br group disappeared. The appearance of new peaks and the disappearance of the C−Br peak evidenced the conversion of $-CH_2Br$ to a quaternary ammonium group. The similar functional groups of I-MPES, I-BPES, and I-QPES are also shown in Figure 5.

3.5. Transmission Electron Microscopy. It has been observed that hydrophilic−hydrophobic multiblock copolymers exhibit well-ordered nanophase separation. It is believed that this separation can provide a co-continuous hydrophilic phase and can facilitate ionic transport. Figure 6 shows the TEM images of the F-QPES and I-QPES multiblock copolymer membranes. The bright and dark regions in the images correspond to unstained hydrophobic domains and tungstate ion-stained electron-rich hydrophilic domains, respectively. Compared with I-QPES (Figure 6a), F-QPES (Figure 6b)

dx.doi.org/10.1021/am5017599 | ACS Appl. Mater. Interfaces 2014, 6, 6776−6785

Table 1. Molecular Weights and Degrees of Bromination of the Block Copolymers

block copolymer	expected $(x + 1)/y$ ratio[a]	obtained $(x + 1)/y$ ratio[b]	M_n (Da)	M_w (Da)	M_w/M_n	bromination degree (%)
F-MPES	1.15:1	1.13:1	159 088	265 086	1.6663	81.41
I-MPES	1.02:1	1.07:1	120 328	202 555	1.6834	82.11

[a]Refers to the value determined by the ratio of the length of oligomer-OH to oligomer-F. [b]Refers to the value from the ^{1}H NMR spectrum of the MPESs; $x + 1$ and y are shown in Scheme 1.

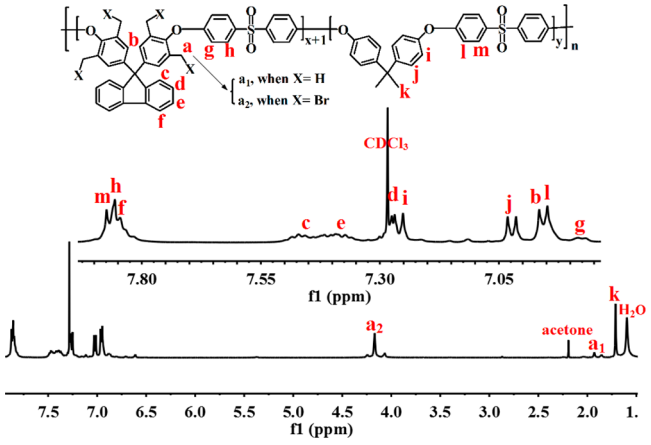

Figure 3. ^{1}H NMR spectrum of the F-BPES block copolymer.

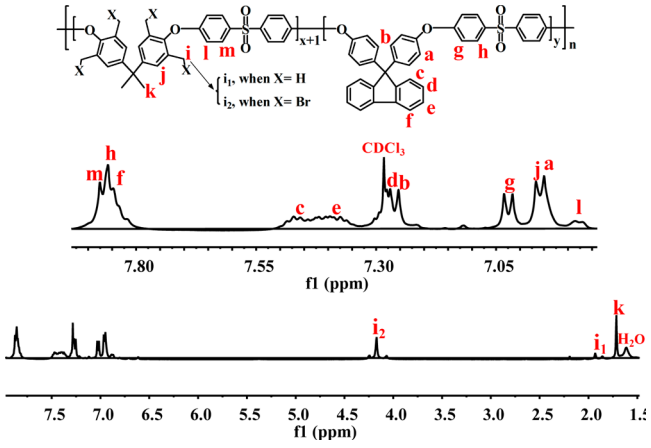

Figure 4. ^{1}H NMR spectrum of the I-QPES block copolymer.

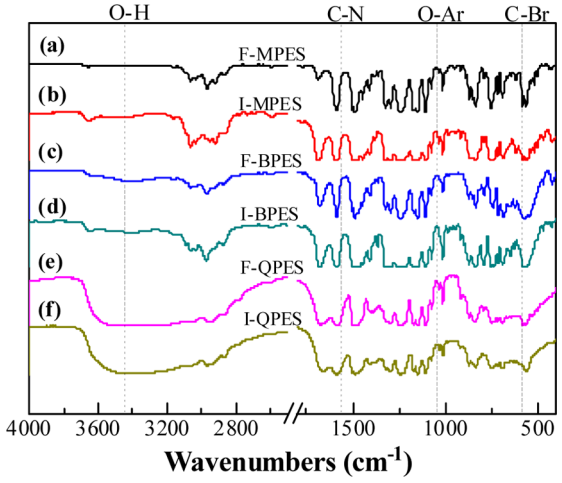

Figure 5. FTIR spectra of (a) F-MPES, (b) I-MPES, (c) F-BPES, (d) I-BPES, (e) F-QPES, and (f) I-QPES.

exhibited much clearer phase-separated structures and formed better interconnected ionic channels, through which OH^- can be transported along the quaternary ammonium groups and water molecules, especially under partially hydrated conditions.

3.6. Small-Angle X-ray Scattering. A morphology with microphase separation is one of the unique properties of block copolymers, and it can be intuitively observed by TEM.[19] However, there is a lack of quantification by this approach. Herein, SAXS was also used to investigate the microphase-separation structure (hydrophilic aggregates) of the QPES membranes. In SAXS, an ionomer peak resulting from the self-assembly of hydrophilic and hydrophobic phases is attributed to the difference in the electron density of the separated phases. SAXS results are presented by plotting the invariant amplitude (Iq^2) as a function of q, as shown in Figure 7. The obvious and sharp peaks indicate the microphase separation generated by the self-assembly of the hydrophilic and hydrophobic phases in the QPES membranes.

From the SAXS profiles, one can infer that a distinct phase separation in the QPES membranes was achieved by the multiblock structure design. For F-QPES and I-QPES, the d_{MAX} values are 9.7 and 8.8 nm, respectively. The size of the hydrophilic aggregates in F-QPES was larger than that in I-QPES. This agrees with the TEM results. The larger hydrophilic aggregates lead to more developed interconnected ion-conducting channels. This can be explained as follows. The illustration of the structure of the QPES membranes is shown in Figure 8. The molecular conformational structure of the sulfone−*co*−fluorene block presents a helical chain shape, and that of the sulfone−*co*−isopropylidene block shows a linear chain shape. With a similar number of hydrophilic groups, the density of the hydrophilic groups on the helical chain is larger than that on the linear chain. By increasing the proportion of the hydrophilic groups, the size of the hydrophilic aggregates increases. As a result, more developed interconnected ion-conducting channels can be further formed.[27]

3.7. Ionic Exchange Capacity, Water Uptake, and Swelling Ratio. The IEC, WU, and SR of the QPES membranes are listed in Table 2. The experimental IEC values of the QPES membranes are in good agreement with the calculated data from the composition of the copolymers and the degree of bromination. This suggests a nearly complete quaternization of the bromobenzyl groups. In terms of the degree of quaternization, F-QPES (96.4%, which refers to the ratio of the experimental IEC values to the calculated ones) was slightly lower than I-QPES (99.5%). This is probably because of the existence of the fluorenyl group in the hydrophilic segment of F-QPES, which could produce a slight steric hindrance to the quaternization reaction. The water uptake of 109.4% at 30 °C and 153.8% at 80 °C for F-QPES (IEC = 1.89 meq·g^{-1}) is higher than the values of 76.1% at 30 °C and 114.2% at 80 °C for I-QPES (IEC = 2.03 meq·g^{-1}). F-QPES showed higher WU than I-QPES at the same temperature, whereas the IEC of F-QPES was slightly lower. This is due to the larger hydrophilic aggregates of the F-QPES membrane.

dx.doi.org/10.1021/am5017599 | ACS Appl. Mater. Interfaces 2014, 6, 6776−6785

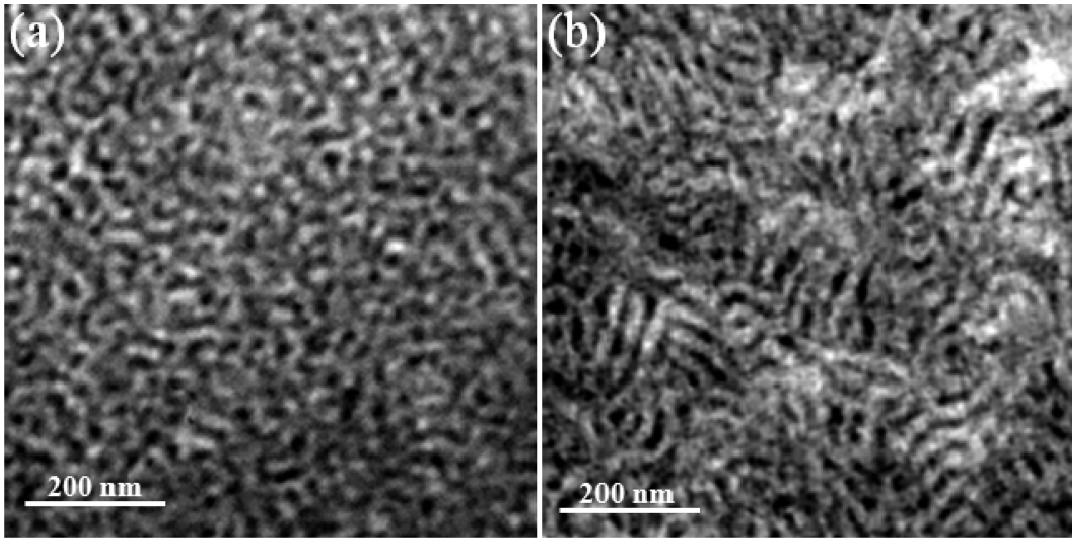

Figure 6. TEM images of I-QPES (a) and F-QPES (b) multiblock copolymer membranes.

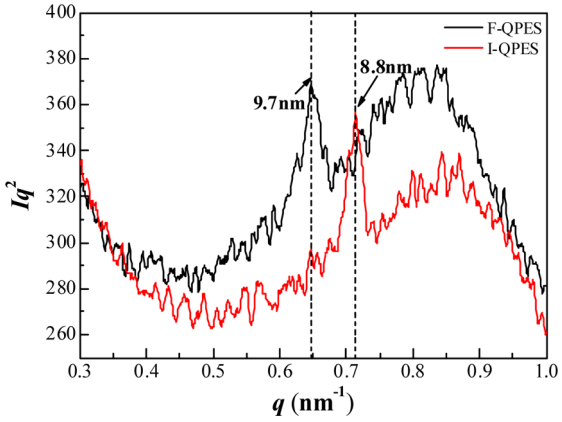

Figure 7. SAXS patterns of the QPES membranes.

Furthermore, it is assumed that water molecules could be accommodated by the interior free volume of the helical chain of the sulfone–*co*–fluorene hydrophilic segment. To our knowledge, the swelling of the hydrophilic membrane results from the weaker cohesion between polymer molecule chains, which is caused by water molecule diffusion between polymer molecule chains. The exact same SR of the QPES membranes (Table 2) could be attributed to a portion of the water molecules being confined by the interior free volume of the helical chain of the sulfone–*co*–fluorene hydrophilic segment instead of diffusing between the molecular chains. The helical chain of the sulfone–*co*–fluorene hydrophobic segment could not operate equally because the hydrophilic group is far from the helical chain.

3.8. Ionic Conductivity. Figure 9a shows the hydroxide ion conductivity of the QPES membranes as a function of temperature at 100% RH. Both of the QPES membranes exhibit considerably high hydroxide conductivities. The ionic conductivity value of F-QPES is 7.46 × 10^{-2} S·cm^{-1} at 30 °C and 19.62 × 10^{-2} S·cm^{-1} at 80 °C, and that of the I-QPES is 6.18 ×10^{-2} at 30 °C and 15.24 × 10^{-2} S·cm^{-1} at 80 °C. Similar to the water uptake, F-QPES showed a higher conductivity than I-QPES under the same conditions. As expected, the more developed interconnected ion-conducting channels are favorable for higher conductivity. Ionic conductivity increased with increasing temperature for both F-QPES and I-QPES because water transfer and ionic conductance are enhanced at higher temperature.

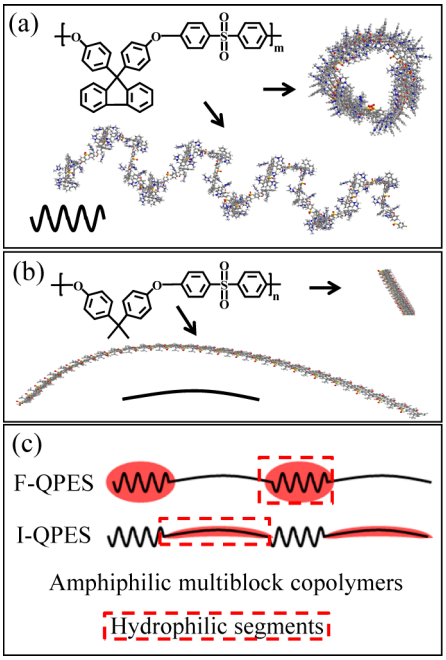

Figure 8. Graphical illustration of the structure of QPES membranes: conformational structure of (a) sulfone–*co*–fluorene block, (b) sulfone–*co*–isopropylidene block, and (c) amphiphilic multiblock copolymers.

3.9. Methanol Permeability. Figure 9b shows the temperature dependence of methanol permeability of the QPES membranes. The methanol permeability of F-QPES and I-QPES was 7.23 and 5.44 ×10^{-8} cm^{-2}·s^{-1} at 30 °C, respectively. The lower methanol permeability of I-QPES than that of F-QPES is caused by the less developed interconnected water channels, which are formed by the hydrophilic aggregates in water. By increasing the temperature, the methanol permeability of the QPES membranes gradually increased. This is largely due to the increasing temperature leading to an intensification of the relaxation of the membrane

dx.doi.org/10.1021/am5017599 | ACS Appl. Mater. Interfaces 2014, 6, 6776–6785

Table 2. Ionic Exchange Capacity, Water Uptake, Swelling Ratio, and Mechanical Properties of the QPES Membranes

	IEC (meq·g^{-1})		WU (%)		SR (%)				
membrane	calcd[a]	exp[b]	30 °C	80 °C	30 °C	80 °C	tensile strength (MPa)	Young's modulus (MPa)	elongation at break (%)
F-QPES	1.96	1.89	109.4	153.8	33.5	53.6	22.59 ± 0.45	310.6 ± 9.3	10.3 ± 0.3
I-QPES	2.04	2.03	76.1	114.2	34.4	61.2	29.89 ± 0.32	241.9 ± 9.7	20.8 ± 0.4

[a]Calculated from the copolymer composition and the degree of bromination. [b]Determined by back titration.

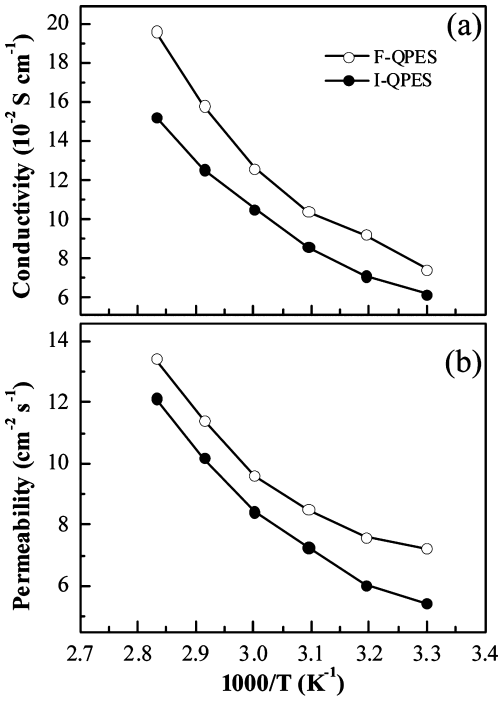

Figure 9. Effect of temperature on the ionic conductivity (a) and methanol permeability (b) of the QPES membranes at 100% RH.

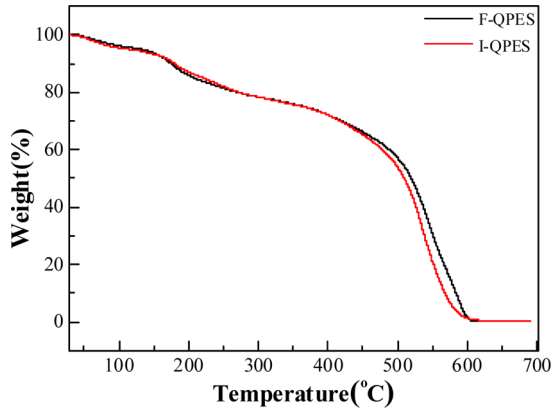

Figure 10. TGA curves of the F-QPES and I-QPES membranes under an air atmosphere.

segment. The free volume therefore increased, resulting in higher methanol permeability.

3.10. Mechanical Property. The mechanical properties of the QPES membranes were studied at room temperature and 60% RH, as shown in Table 2. The F-QPES membrane showed both weaker tensile strength and elongation at break than the I-QPE membrane. These results are reasonable when considering that although they have almost the same swelling ratio, the former has a higher WU than the latter and the water could act as a plasticizer in the membranes.[28] Both of the QPES membranes showed high mechanical strength because of their robust backbone structure.

3.11. Thermal Stability. Figure 10 shows the thermal degradation behavior of OH^- form F-QPES and I-QPES evaluated via TGA under an air atmosphere. Both F-QPES and I-QPES have almost the same tendency. The decomposition process of the membranes showed a three-step weight loss. The first weight loss (less than 5%), occurring at 30−180 °C, was mainly assigned to the evaporation of the bonded water and the residual solvent (NMP) in the membranes. The second weight loss, from 180 to 300 °C, was attributed to the decomposition of the methyl quaternary ammonium salt group. The third weight loss, around 500 °C, was assigned to the cleavage of the polymer main chain. As mentioned earlier, the resulting alkaline membranes exhibit good thermal stability at an intermediate temperature under an air atmosphere.

3.12. Scanning Electron Microscopy. Figure 11 shows the SEM images of the F-QPES and I-QPES membranes. A thickness of approximately 40 μm was observed from the cross-sectional view (Figure 11a,b). A homogeneous, smooth, and dense surface structure is also displayed (Figure 11c,d). The smooth surface of the membranes leads to an effective contact area and results in a high catalytic efficiency. The dense surface structure of the membranes can effectively reduce the permeability of methanol. In other words, the homogeneous and dense AEMs can exhibit good performance in DMFCs in terms of their catalytic efficiency and methanol resistance.

3.13. Alkaline Stability. The QPES membranes were soaked in a 2 M NaOH solution at 60 °C to evaluate their alkaline stability. The time dependence of the IEC and ionic conductivity were both studied. As can be seen in Figure 12, an initial sharp decrease in both the IEC and ionic conductivity was observed after the membrane samples were immersed in alkaline media for 196 h, after which time the IEC and ionic conductivity tended to present a constant value. After being treated in a 2 M NaOH solution at 60 °C for 480 h, F-QPES showed a better alkaline stability than I-QPES. The former still retained about an 80% IEC value (1.52 meq·g^{-1}) and a 72% ionic conductivity value (5.37×10^{-2} S·cm^{-1}). The latter kept the corresponding values of 69% (1.40 meq·g^{-1}) and 61% (3.76×10^{-2} S·cm^{-1}). For F-QPES, it is assumed that the stability of quaternary ammonium groups was enhanced by the presence of the helical sulfone−*co*−fluorene molecular conformational structure, which could hinder the attack by hydroxyl ions because of the high steric bulk.

4. CONCLUSIONS

With a nearly identical backbone, two kinds of novel aromatic multiblock PES AEMs, in which the fluorene−sulfone segment was alternatively treated as hydrophilic and hydrophobic, were designed and synthesized via block copolycondensation of corresponding telechelicoligomers, bromination, quaternization, and ion-exchange reactions. Both of the QPES membranes

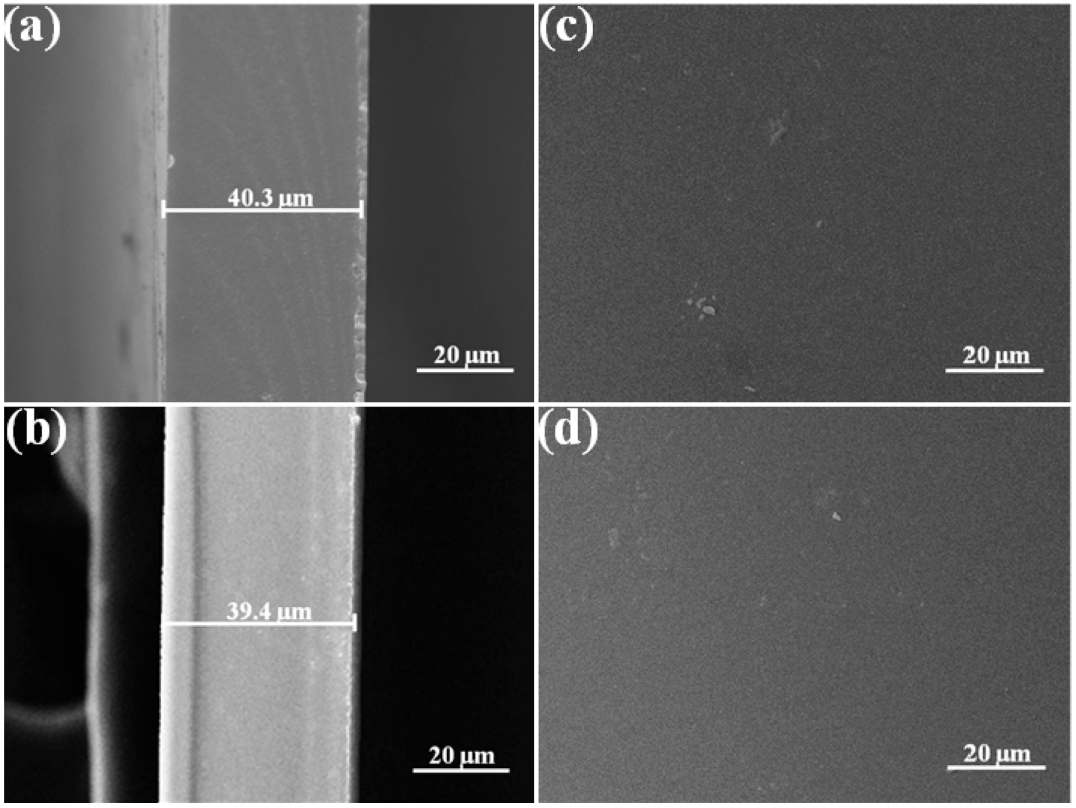

Figure 11. SEM images of the F-QPES (a, c) and I-QPES (b, d) membranes.

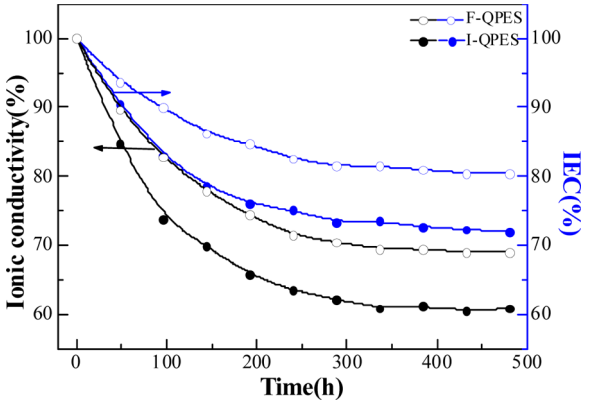

Figure 12. Alkaline stability of the QPES membranes in a 2 M NaOH solution at 60 °C.

showed distinct hydrophilic/hydrophobic phase separation to form transport channels for OH^- diffusion, as confirmed by SAXS and TEM analysis. The size of the hydrophilic aggregates in F-QPES (9.7 nm) was larger than that in I-QPES (8.8 nm) and thus it formed more developed ion-conducting channels. F-QPES showed higher WU and ionic conductivity as well as better mechanical properties and alkaline stability than I-QPES, but it demonstrated a worse methanol barrier performance than I-QPES. It is more effective to utilize the fluorene−sulfone segment as the hydrophilic segment than as the hydrophobic segment to improve the ionic conductivity and alkali resistance of AEMs.

■ ASSOCIATED CONTENT

Supporting Information

^{1}H NMR spectra of the oligomers, and the length and molecular weight of the oligomers. This material is available free of charge via the Internet at http://pubs.acs.org.

■ AUTHOR INFORMATION

Corresponding Author

*E-mail: qlliu@xmu.edu.cn; Tel.: 86-592-2188072; Fax: 86-592-2184822.

Notes

The authors declare no competing financial interest.

■ ACKNOWLEDGMENTS

Financial support from the National Nature Science Foundation of China (grant nos. 21376194 and 21076170), the Nature Science Foundation of Fujian Province of China (grant no. 2009J01040), and the research fund for the Priority Areas of Development in Doctoral Program of Higher Education (no. 20130121130006) is gratefully acknowledged. TEM characterization provided from Professor Lin Zhang at Zhejiang University is also appreciated. We are very thankful for the referees' helpful comments.

■ REFERENCES

(1) *Handbook of Fuel Cells: Fundamentals Technology and Applications*; Vielstich, W., Lamm, A., Gasteiger, H. A., Eds.; Wiley: Chichester, England, 2003.

(2) Mauritz, K. A.; Moore, R. B. State of Understanding of Nafion. *Chem. Rev.* **2004**, *104*, 4535−4586.

(3) Hickner, M. A.; Ghassemi, H.; Kim, Y. S.; Einsla, B. R.; McGrath, J. E. Alternative Polymer Systems for Proton Exchange Membranes (PEMs). *Chem. Rev.* **2004**, *104*, 4587−4612.

(4) Varcoe, J. R.; Slade, R. C. Prospects for Alkaline Anion Exchange Membranes in Low Temperature Fuel Cells. *Fuel Cells* **2005**, *5*, 187−200.
(5) Wasmus, S.; Küver, A. J. Methanol Oxidation and Direct Methanol Fuel Cells: A Selective Review. *Electroanal. Chem.* **1999**, *461*, 14−31.
(6) Sanabria-Chinchilla, J.; Asazawa, K.; Sakamoto, T.; Yamada, K.; Tanaka, H.; Strasser, P. Noble Metal-Free Hydrazine Fuel Cell Catalysts: EPOC Effect in Competing Chemical and Electrochemical Reaction Pathways. *J. Am. Chem. Soc.* **2011**, *133*, 5425−5431.
(7) Olson, T. S.; Pylypenko, S.; Atanassov, P.; Asazawa, K.; Yamada, K.; Tanaka, H. Anion-Exchange Membrane Fuel Cells: Dual-Site Mechanism of Oxygen Reduction Reaction in Alkaline Media on Cobalt−Polypyrrole Electrocatalysts. *J. Phys. Chem. C* **2010**, *114*, 5049−5059.
(8) Wang, F.; Hickner, M.; Kim, Y. S.; Zawodzinski, T. A.; McGrath, J. E. Direct Polymerization of Sulfonated Poly(arylene ether sulfone) Random (Statistical) Copolymers: Candidates for New Proton Exchange Membranes. *J. Membr. Sci.* **2002**, *197*, 231−242.
(9) Zhang, F.; Zhang, H.; Qu, C. Imidazolium Functionalized Polysulfone Anion Exchange Membrane for Fuel Cell Application. *J. Mater. Chem.* **2011**, *21*, 12744−12752.
(10) Zhao, C. H.; Gong, Y.; Liu, Q. L.; Zhang, Q. G.; Zhu, A. M. Self-Crosslinked Anion Exchange Membranes by Bromination of Benzylmethyl-Containing Poly(sulfone)s for Direct Methanol Fuel Cells. *Int. J. Hydrogen Energy* **2012**, *37*, 11383−11393.
(11) Lin, X.; Wu, L.; Liu, Y.; Ong, A. L.; Poynton, S. D.; Varcoe, J. R.; Xu, T. Alkali Resistant and Conductive Guanidinium-Based Anion-Exchange Membranes for Alkaline Polymer Electrolyte Fuel Cells. *J. Power Sources* **2012**, *217*, 373−380.
(12) Wang, J.; Zhao, Z.; Gong, F.; Li, S.; Zhang, S. Synthesis of Soluble Poly(arylene ether sulfone) Ionomers with Pendant Quaternary Ammonium Groups for Anion Exchange Membranes. *Macromolecules* **2009**, *42*, 8711−8717.
(13) Zhou, J.; Unlu, M.; Vega, J. A.; Kohl, P. A. Anionic Polysulfone Ionomers and Membranes Containing Fluorenyl Groups for Anionic Fuel Cells. *J. Power Sources* **2009**, *190*, 285−292.
(14) Wang, C.; Shin, D. W.; Lee, S. Y.; Kang, N. R.; Robertson, G. P.; Lee, Y. M.; Guiver, M. D. A Clustered Sulfonated Poly(ether sulfone) Based on a New Fluorene-Based Bisphenol Monomer. *J. Mater. Chem.* **2012**, *22*, 25093−25101.
(15) Bae, B.; Miyatake, K.; Watanabe, M. Synthesis and Properties of Sulfonated Block Copolymers Having Fluorenyl Groups for Fuel-Cell Applications. *ACS Appl. Mater. Interfaces* **2009**, *1*, 1279−1286.
(16) Bae, B.; Miyatake, K.; Watanabe, M. Sulfonated Poly(arylene ether sulfone ketone) Multiblock Copolymers with Highly Sulfonated Block. Synthesis and Properties. *Macromolecules* **2010**, *43*, 2684−2691.
(17) Bae, B.; Hoshi, T.; Miyatake, K.; Watanabe, M. Sulfonated Block Poly(arylene ether sulfone) Nembranes for Fuel Cell Applications via Oligomeric Sulfonation. *Macromolecules* **2011**, *44*, 3884−3892.
(18) Wang, C.; Li, N.; Shin, D. W.; Lee, S. Y.; Kang, N. R.; Lee, Y. M.; Guiver, M. D. Fluorene-Based Poly(arylene ether sulfone)s Containing Clustered Flexible Pendant Sulfonic Acids as Proton Exchange Membranes. *Macromolecules* **2011**, *44*, 7296−7306.
(19) Tanaka, M.; Fukasawa, K.; Nishino, E.; Yamaguchi, S.; Yamada, K.; Tanaka, H.; Bae, B.; Miyatake, K.; Watanabe, M. Anion Conductive Block Poly(arylene ether)s: Synthesis, Properties, and Application in Alkaline Fuel Cells. *J. Am. Chem. Soc.* **2011**, *133*, 10646−10654.
(20) Tanaka, M.; Koike, M.; Miyatake, K.; Watanabe, M. Anion Conductive Aromatic Ionomers Containing Fluorenyl Groups. *Macromolecules* **2010**, *43*, 2657−2659.
(21) Tanaka, M.; Koike, M.; Miyatake, K.; Watanabe, M. Synthesis and Properties of Anion Conductive Ionomers Containing Fluorenyl Groups for Alkaline Fuel Cell Applications. *Polym. Chem.* **2011**, *2*, 99−106.
(22) Miyatake, K.; Bae, B.; Watanabe, M. Fluorene-Containing Cardo Polymers as Ion Conductive Membranes for Fuel Cells. *Polym. Chem.* **2011**, *2*, 1919−1929.
(23) Fujii, K.; Hata, S.; Fukui, K.; Kato, H.; Numata, Y. Method for Producing Fluorene Derivative. WO Patent 2,010,119,727, 2010.
(24) Komkova, E.; Stamatialis, D.; Strathmann, H.; Wessling, M. Anion Exchange Membranes Containing Diamines: Preparation and Stability in Alkaline Solution. *J. Membr. Sci.* **2004**, *244*, 25−34.
(25) Bae, B.; Yoda, T.; Miyatake, K.; Uchida, H.; Watanabe, M. Proton Conductive Aromatic Ionomers Containing Highly Sulfonated Blocks for High Temperature Operable Fuel Cells. *Angew. Chem., Int. Ed.* **2010**, *122*, 327−330.
(26) Guo, T. Y.; Zeng, Q. H.; Zhao, C. H.; Liu, Q. L.; Zhu, A. M.; Broadwell, I. Quaternized Polyepichlorohydrin/PTFE Composite Anion Exchange Membranes for Direct Methanol Alkaline Fuel Cells. *J. Membr. Sci.* **2011**, *371*, 268−275.
(27) Chen, D.; Wang, S.; Xiao, M.; Meng, Y.; Hay, A. S. Novel Polyaromatic Ionomers with Large Hydrophilic Domain and Long Hydrophobic Chain Targeting at Highly Proton Conductive and Stable Membranes. *J. Mater. Chem.* **2011**, *21*, 12068−12077.
(28) Chen, D.; Hickner, M. A.; Wang, S.; Pan, J.; Xiao, M.; Meng, Y. Synthesis and Characterization of Quaternary Ammonium Functionalized Fluorene-Containing Cardo Polymers for Potential Anion Exchange Membrane Water Electrolyzer Applications. *Int. J. Hydrogen Energy* **2012**, *37*, 16168−16176.